ETH ZÜRICH

DEPARTMENT OF PHYSICS
TRAPPED ION QUANTUM INFORMATION GROUP

Semester project report

Coupling of Ion Oscillation and Optical Cavity Modes

Author
Andraz Omahen

Supervisors
Dr. Thanh Long Nguyen
Martin Wagener

Group leader
Prof. Dr. Jonathan Home

October 2021

Abstract

A promising way to implement fault-tolerant quantum computing is to encode qubit information in more dimensional physical systems such as harmonic oscillators. We investigate dispersive coupling between two such oscillators: the motion of an ion in a harmonic trap and an optical cavity. The interaction is achieved by using an internal electrical transition of the ion driven by a coherent light field. Such coupling effectively produces a beamsplitter interaction between the two oscillators. We show that energy levels are modified by a stark shift (which has to be taken into account if we want that state transfer between cavity and motion has high fidelity). We furthermore explore interaction between individual optical cavities coupled via a running light field. Such a coupling could be used to transfer quantum states from the motion of an ion in one cavity to a distant cavity and ultimately to another ion in that cavity.

Contents

1 Introduction

Motional states of ions trapped in harmonic potentials offer various possibilities for creation and study of nonclassical states [1, 2, 3] as well as quantum computing [4] (which includes actions such as performing CNOT gate [5], initializing the qubit state [6], entanglement of two trapped ions [7]). Moreover, motional modes can be used for quantum error correction protocols. Detection and correction of inevitable quantum errors demand redundancy, which can be conveniently encoded on the state of a harmonic oscillator [8, 9, 10]. An example of a code that encodes qubits by utilizing many dimensions of one physical system is cat code (which can protect against photon loss) [11]. A more universal approach is the Gottesman, Kitaev, Preskill (GKP) code [12], which can correct all single qubit errors. However, for building a quantum computer, we need communication (coupling) between many physical qubits. This can be achieved by joining spatially separated ions in one common trap using electric fields (QCCD architecture [13]). An alternative approach would be the use of photons as intermediary link between qubits, as proposed by Parkins and Kimble [14]. For this we firstly need to put a trapped ion in an optical cavity and investigate a simple state transfer between cavity and motional modes. Once we understand this process, two such systems (oscillating ions inside the cavity) could be coupled via decay from one cavity to another, since we already know how to transfer a state from cavity to motion.

The aim of this report will be to simulate state transfer between optical cavity and motional modes of a trapped ion while reproducing the results (but using a different approach) from Parkins and Kimble [14] so that we can also elaborate on them. We start by describing the system relevant for state transfer and perform Schrieffer-Wolf transformation. To learn more about our Hamiltonian we simulate transfer of a Fock and cat state and notice previously derived Stark shift due to coupling of cavity and motion. Later, we expand our system by adding a second cavity which decays into the first cavity. This enables us to simulate state transfer from second cavity to the motion of the ion. An intuitive further step is to put an ion in the second cavity and study communication between different motional qubits, however, this is a topic of future investigations.

2 Model description

Our model consists of a two-level ion (or atom) confined in a harmonic trap. Atomic levels are separated by frequency ω_a and are coupled via a Jaynes-Cummings interaction to an optical cavity at frequency ω_c. Furthermore, the atomic transition is driven by an external laser field of frequency ω_L. The system is shown on Figure 1. We describe our system in the interaction picture with respect to $\hbar\omega_L a^\dagger a + \hbar\omega_L \sigma_+\sigma_-$ and perform a rotating-wave approximation where we assume that we are interested in timescales much bigger than $1/\omega_L$. This means that we can neglect fast rotating terms which come from coupling of cavity to the atom: $\left(\hat{\sigma}_+ \mathrm{e}^{\mathrm{i}\omega_L t} + \hat{\sigma}_- e^{-\mathrm{i}\omega_L t}\right)$ and $\left(\hat{a}^\dagger\hat{\sigma}_+ e^{2\mathrm{i}\omega_L t} + \hat{a}\hat{\sigma}_- e^{-2\mathrm{i}\omega_L t}\right)$, because they oscillate quickly compared to $\left(\hat{a}\hat{\sigma}_+ + \hat{a}^\dagger\hat{\sigma}_-\right)$ in our reference frame. The resulting Hamiltonian is [14]:

$$\hat{H} = \sum_{i=x,y,z} \hbar\nu_i \left(\hat{b}_i^\dagger \hat{b}_i + \frac{1}{2}\right) + \hbar\delta\hat{a}^\dagger\hat{a} + \hbar\Delta\hat{\sigma}_+\hat{\sigma}_- + \hbar\left[\varepsilon_L\left(\hat{x},\hat{y},\hat{z}\right)\hat{\sigma}_+ + \varepsilon_L\left(\hat{x},\hat{y},\hat{z}\right)^*\hat{\sigma}_-\right] + \hbar g_0 \sin\left(k\hat{x}\right)\left(\hat{a}\hat{\sigma}_+ + \hat{a}^\dagger\hat{\sigma}_-\right) \tag{1}$$

where ν_i is the trap frequency in direction $i = x, y, z$. $\hat{a}$ and $\hat{b}_i$ are annihilation operators for cavity field and harmonic motion respectively while $\hat{\sigma}_-$ is the lowering operator of the two-level ion. $\delta = \omega_c - \omega_L$ is the difference between cavity and laser frequency and similarly $\Delta = \omega_a - \omega_L$ denotes the difference between atom and laser frequency. We will select our frequencies such that the motional and cavity excitations have the same energy in the interaction picture. This condition will be determined later, but it approximately holds:

$$\nu \approx \delta = \omega_c - \omega_L. \tag{2}$$

The energy levels in our system are shown on the right side of Figure 1 where one can observe that δ and ν fulfill the approximate condition in equation (2). The amplitude of the laser electric field is denoted by $\varepsilon_L(\hat{x},\hat{y},\hat{z})$. If the laser beam size is much larger than the ionic wave packet size, we can assume that laser electric field is constant: $\varepsilon_L(\hat{x},\hat{y},\hat{z}) = \varepsilon_L$. The cavity-atom dipole coupling strength is given by g_0 and the sine function describes the standing wave structure of the cavity electric field. Here we made an assumption that the center of the trap is located at a node of the cavity field, with $k = 2\pi/\lambda$ being the wavenumber and $\hat{x} = \sqrt{\hbar/2m\nu}\left(\hat{b}+\hat{b}^\dagger\right)$ the ion position operator, where m is the mass of the ion. If the center of the trap was located at an anti-node, we would have used a cosine function.

We will work in the Lamb-Dicke limit and assume the size of the ionic wavepacket (in all directions) is small compared with the optical wavelength of light in cavity (λ), which means that we can do an expansion: $\sin(k\hat{x}) \simeq k\hat{x} = \eta\left(\hat{b}+\hat{b}^\dagger\right)$. Here $\eta \ll 1$ is the Lamb-Dicke parameter. If the optical cavity couples to only one mode of motion, the problem becomes one-dimensional and we only have one frequency (ν) and one motional annihilation operator $\left(\hat{b}\right)$ despite having a three dimensional trap. We arrive to:

$$\hat{H} = \hbar\nu\left(\hat{b}^\dagger\hat{b}+\frac{1}{2}\right) + \hbar\delta\hat{a}^\dagger\hat{a} + \hbar\Delta\hat{\sigma}_+\hat{\sigma}_- + \hbar\varepsilon_L\left[\hat{\sigma}_+ + \hat{\sigma}_-\right] + \hbar g_0\eta\left(\hat{b}+\hat{b}^\dagger\right)\left(\hat{a}\hat{\sigma}_+ + \hat{a}^\dagger\hat{\sigma}_-\right). \qquad (3)$$

With this Hamiltonain we will simulate transfer of a cavity state to the motional mode of the ion. The terms that are responsible for state transfer come from the last term in equation (3) and are of the form $\hat{a}\hat{b}^\dagger + \hat{a}^\dagger\hat{b}$ meaning that they create one excitation in motional mode on account of annihilating a quantum of energy from cavity and vice versa. The interacting terms can be resonantly driven by selecting appropriate frequencies Δ, ν and δ which will be shown in the next section.

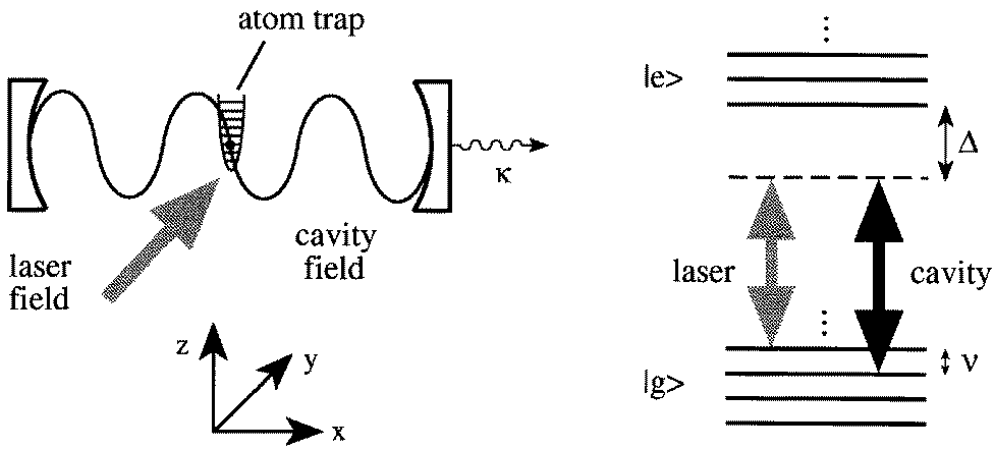

Figure 1: Sketch of our system of interest: a two-level ion (or atom) is trapped inside a harmonic potential. The cavity is aligned along the $x-$axis, while the laser is incident from a direction in the $y-z$ plane. The two atomic levels are coupled to a laser field and a single mode of an optical cavity. Initially, we assume that the cavity decay rate κ is zero. On the right side, we can see energy levels of our system in the interaction picture.
Taken from [14].

3 Schrieffer-Wolf transformation

We notice that our equation (3) is of the form: $\hat{H} = \hat{H}_0 + \hat{H}_I$. Here $H_0 = \hbar\nu\left(\hat{b}^\dagger\hat{b} + \frac{1}{2}\right) + \hbar\delta\hat{a}^\dagger\hat{a} + \hbar\Delta\hat{\sigma}_+\hat{\sigma}_-$ describes the system without coupling, while all the interaction terms are described by $\hat{H}_I = \hbar\varepsilon_L\left[\hat{\sigma}_+ + \hat{\sigma}_-\right] + \hbar g_0\eta\left(\hat{b} + \hat{b}^\dagger\right)\left(\hat{a}\hat{\sigma}_+ + \hat{a}^\dagger\hat{\sigma}_-\right)$. If the term $\hat{H}_I$ is small compared to $\hat{H}_0$, we can approximate our Hamiltonian up to third order in $\hat{H}_I$ by doing a Schrieffer-Wolf transformation [15, 16]. After writing our Hamiltonian in a different basis ("dressed" state basis): $\hat{H}' = \exp\left(\hat{S}\right)\hat{H}\exp\left(-\hat{S}\right)$ and conveniently choosing an anti-Hermitian $\hat{S}$ of the form:

$$\hat{S} = g_0\eta\left(\frac{\hat{a}^\dagger\hat{b}\hat{\sigma}_-}{-\nu+\delta-\Delta} - \frac{\hat{a}\hat{b}^\dagger\hat{\sigma}_+}{-\nu+\delta-\Delta} + \frac{\hat{a}^\dagger\hat{b}^\dagger\hat{\sigma}_-}{\nu+\delta-\Delta} - \frac{\hat{a}\hat{b}\hat{\sigma}_+}{\nu+\delta-\Delta}\right) + \frac{\varepsilon_L}{\Delta}\left(\hat{\sigma}_+ - \hat{\sigma}_-\right), \tag{4}$$

we arrive at an approximate Hamiltonian:

$$\hat{H}' = \hat{H}_0 + \frac{1}{2}\left[\hat{S}, \hat{H}_I\right] + O\left(\left[\hat{S}, \left[\hat{S}, \hat{H}_I\right]\right]\right). \tag{5}$$

Caution is needed when neglecting higher order Schrieffer-Wolf terms, namely $\left[\hat{S}, \left[\hat{S}, \hat{H}_I\right]\right]$. This means that we should be aware of possible divergences at $\Delta = \delta \pm \nu$. Furthermore to neglect higher order terms produced by $\hat{S}_{RSB} = g_0\eta\left(\frac{\hat{a}^\dagger\hat{b}\hat{\sigma}_-}{-\nu+\delta-\Delta} - \frac{\hat{a}\hat{b}^\dagger\hat{\sigma}_+}{-\nu+\delta-\Delta}\right)$ the coefficient $(g_0\eta)^3/(-\nu+\delta-\Delta)^2 \propto \left[\hat{S}_{RSB}, \left[\hat{S}_{RSB}, \hat{H}_I\right]\right]$ needs to be small, which we should keep in mind when selecting Δ. Similar consideration holds for other terms in $\hat{S}$.

The first two terms in equation (4) are the red sideband terms and are resonant when $\delta = \nu$, while third and fourth terms represent blue sideband with resonance at $\delta = -\nu$. The resonance condition comes from going into the interaction picture with respect to bare Hamiltonians of cavity and harmonic oscillator $\left(\hbar\nu\hat{b}^\dagger\hat{b} + \hbar\delta\hat{a}^\dagger\hat{a}\right)$ and neglecting time dependent terms. We select $\delta = \nu$ which means that only the first, second and fifth term in equation (4) contribute significantly to the commutator $[S, H_I]$ in equation (5). Additionally, we assume that the atom starts the ground state. We arrive at the Hamiltonian (up to a constant factor):

$$\hat{H}' = H_0 + \frac{1}{2}\left[g_0\eta\left(\frac{\hat{a}^\dagger\hat{b}\hat{\sigma}_-}{-\Delta} - \frac{\hat{a}\hat{b}^\dagger\hat{\sigma}_+}{-\Delta}\right) + \frac{\varepsilon_L}{\Delta}\left(\hat{\sigma}_+ - \hat{\sigma}_-\right), \hat{H}_I\right] =$$

$$\hat{H}' = \hbar\nu\left(\hat{b}^\dagger\hat{b} + \frac{1}{2}\right) + \hbar\left(\delta - \frac{g_0^2\eta^2}{\Delta}\right)\hat{a}^\dagger\hat{a} - \hbar\Omega\left(\hat{a}^\dagger\hat{b} + \hat{a}\hat{b}^\dagger\right) - \frac{\hbar g_0^2\eta^2}{\Delta}\hat{a}^\dagger\hat{a}\hat{b}^\dagger\hat{b} - \frac{1}{2}\frac{\hbar g_0^2\eta^2}{2\Delta}\hat{a}^\dagger\hat{a}\left(\hat{b}^2 + \left(\hat{b}^\dagger\right)^2\right) \tag{6}$$

with Rabi frequency Ω of cavity-motion coupling defined as:

$$\Omega = \frac{g_0\eta\varepsilon_L}{\Delta}. \tag{7}$$

In equation (6) we can see that the third term resembles a beamsplitter where the two input modes are cavity field and motional modes of the ion (alternative derivation of the beamsplitter interaction is in [14]). The second terms tells us about the stark shift of cavity levels if the initial state of motion is the ground state. The cavity is shifted by $-\hbar g_0^2\eta^2/\Delta$ and consequently we have to tune the laser to:

$$\delta = \nu + \frac{(g_0\eta)^2}{\Delta} \tag{8}$$

if we want the cavity and motion to be in resonance. If the initial state of one of the subsystems (motion in our case) is not the ground state, the fourth term in equation (6) is significant and our prediction (8) is wrong. We would have to adjust the detuning according to the motional occupation as described in the fourth term. The last term describes double excitations and deexcitations of motional modes depending on occupation of cavity. They contribute to lower fidelities.

We still have to look at the remaining terms in H' which come from the blue sideband terms. They produce anti-Jaynes-Cummings interaction together with Stark shift. Both can be neglected when $\delta = \nu$ (because they rotate quickly with time in the interaction picture with respect to bare cavity and motional Hamiltonian):

$$\begin{aligned}\hat{H}'_{BSB} &= \frac{1}{2}\left[g_0\eta\left(\frac{\hat{a}^\dagger\hat{b}^\dagger\hat{\sigma}_-}{2\delta-\Delta} - \frac{\hat{a}\hat{b}\hat{\sigma}_+}{2\delta-\Delta}\right), \hat{H}_I\right] \\ &= -\frac{1}{2}\hbar g_0\eta\epsilon_L\left(\frac{1}{\Delta}+\frac{1}{\Delta-2\delta}\right)\left(\hat{a}\hat{b}+\hat{a}^\dagger\hat{b}^\dagger\right) - \frac{\hbar g_0^2\eta^2}{\Delta-2\delta}\hat{a}^\dagger\hat{a}\hat{b}^\dagger\hat{b} - \frac{1}{2}\frac{\hbar g_0^2\eta^2}{\Delta-2\delta}\hat{a}^\dagger\hat{a}\left(\hat{b}^2+\left(\hat{b}^\dagger\right)^2\right). \quad (9)\end{aligned}$$

These terms reduce the fidelity of our state transfer. The first term does not transfer excitations from cavity to motion, but either creates or annihilates one excitation in both cavity and motion. Another effect which can reduce our fidelity is the stark shift described by the second term, but we can take it into account when tuning parameter δ. We neglect it in our simulations because it is small (of the second order in η and time dependent). The last term creates or annihilates two quanta of energy analogously to the last red sideband term (but with $\Delta - 2\delta$ instead of Δ).

To sum up, lower fidelities are produced by off-resonant excitation of blue sideband Hamiltonian, which can be suppressed by enhancing $\delta = \nu$ resulting in faster rotations. The second source of errors are the terms that destroy our motional state: $\eta^2\left(\hat{b}^2+\left(\hat{b}^\dagger\right)^2\right)$ and can be reduced by making the Lamb-Dicke parameter (η) smaller. This also makes $\Omega \sim \eta$ smaller which means that state transfer takes longer, but the fidelities are better. Finally, higher order terms in the Schrieffer-Wolf transformation $\left(1/2\cdot\left[\hat{S},\left[\hat{S},\hat{H}_I\right]\right]+...\right)$ also contribute to the transformed Hamiltonian and can be diminished by lowering η and increasing Δ.

4 Simulations of state transfer between cavity and motion

To gain a better understanding of a rather complicated Hamiltonian in equation (3) (or in equations (6) and (9)), which couples three systems, we will perform some simulations with the Python package Qutip [17]. We will explore different characteristics of our system (oscillations of occupation numbers, AC stark shift of energy levels, beamsplitter interaction between cavity and motional modes) under time evolution of various initial states.

4.1 Fock states

We will start by analyzing the evolution of Fock states for which we expect energy transfer between cavity and motional excitations. The system parameters in our simulation are: $\delta = 2\cdot 2\pi s^{-1}$, $\Delta = 20\cdot 2\pi s^{-1}$, $\nu = 2\cdot 2\pi s^{-1}$, $g_0 = 0.25\cdot 2\pi s^{-1}$, $\varepsilon_L = 1\cdot 2\pi s^{-1}$, $\eta = 0.1$, $\hbar = 1$. Our initial state is $|\psi_0\rangle = |5\rangle_{cavity}\otimes|0\rangle_{atom}\otimes|0\rangle_{motion}$, where $|N\rangle$ denotes a Fock state N. The calculated expected occupation numbers of atom, cavity and motion versus dimensionless time $\tau = t\Omega/\pi$ (with $\Omega = g_0\eta\varepsilon_L/\Delta$ being the Rabi frequency of cavity-motion coupling derived defined in equation (7)) can be seen in Figure 2.

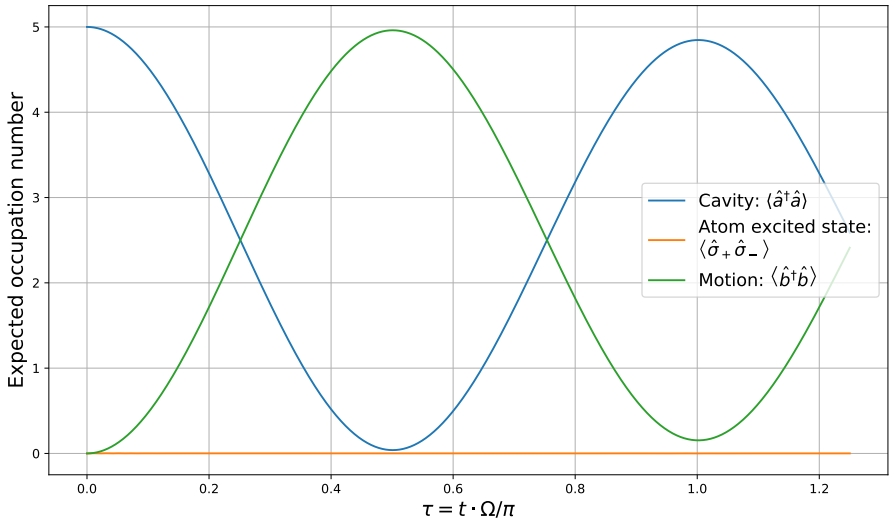

Figure 2: Exchange of energy between cavity and motional modes in the system initialized in state: $|\psi_0\rangle = |5\rangle_{cavity} \otimes |0\rangle_{atom} \otimes |0\rangle_{motion}$.

We can notice that at $\tau = 0.5$ the whole population is not transferred from cavity to motion and similarly at $\tau = 1$ the transfer back to cavity is not perfect. The reason is that the eigenenergies of our system become slightly modified due to the interaction between subsystems as derived in section 3. This phenomenon is called the AC Stark shift [18]. Consequently $\delta = \nu$ as proposed in equation (2) is not the resonant case. This can be seen in Figure 3 where we plot the highest achieved occupation of the motional mode versus the normalized detuning of cavity: $\delta/\nu - 1$. The peak is not at $\delta/\nu - 1 = 0$, as one might naively expect by equating cavity and motional energies in equation (3), but rather at some $\delta/\nu - 1 > 0$.

In Figure 3 we only looked at expected population of states. We ignored the distribution of population over different Fock states (e.g. Fock state one and coherent state one have the same expectation number but different distribution over Fock states) and that quantum states also have phases. Both phases and distribution over Fock states can be taken into account by looking at fidelity of state transfer. For density matrices ρ, σ it is defined as:

$$\mathcal{F}(\rho, \sigma) = \left(\mathrm{tr} \sqrt{\sqrt{\rho} \sigma \sqrt{\rho}} \right)^2 . \tag{10}$$

For pure states equation (10) simplifies to:

$$\mathcal{F}(\rho, \sigma) = \left| \langle \psi_{rho} | \psi_\sigma \rangle \right|^2 . \tag{11}$$

We look at maximum fidelity of state transfer $\mathcal{F}\left(\rho_m, \rho_{c,0}\right)$, which means that we compare the motional density matrix with the highest motional occupation number ρ_m and the cavity density matrix at time zero $\rho_{c,0}$. We get a partial density matrix of a subsystem by tracing out components of the full system. For example, we get $\rho_{c,0}$ by tracing out motional modes and spin: $\rho_{c,0} = \mathrm{tr}_{spin,\, motion}\left(|\psi_0\rangle \langle \psi_0| \right)$. We then plot $\mathcal{F}\left(\rho_m, \rho_{c,0}\right)$ with respect to $\delta/\nu - 1$ in Figure 4. The highest fidelity is at $\delta/\nu - 1 > 0$ and is lower than one, which can be expected because the transfer of energy quanta is not perfect. Based on the derivation and discussion in section 3, this comes from higher order terms in Schrieffer-Wolf transformation, off-resonant excitation of the blue sideband and motional relaxation terms produced by the red sideband which include $\left(\hat{b}^2 + \left(\hat{b}^\dagger \right)^2 \right)$.

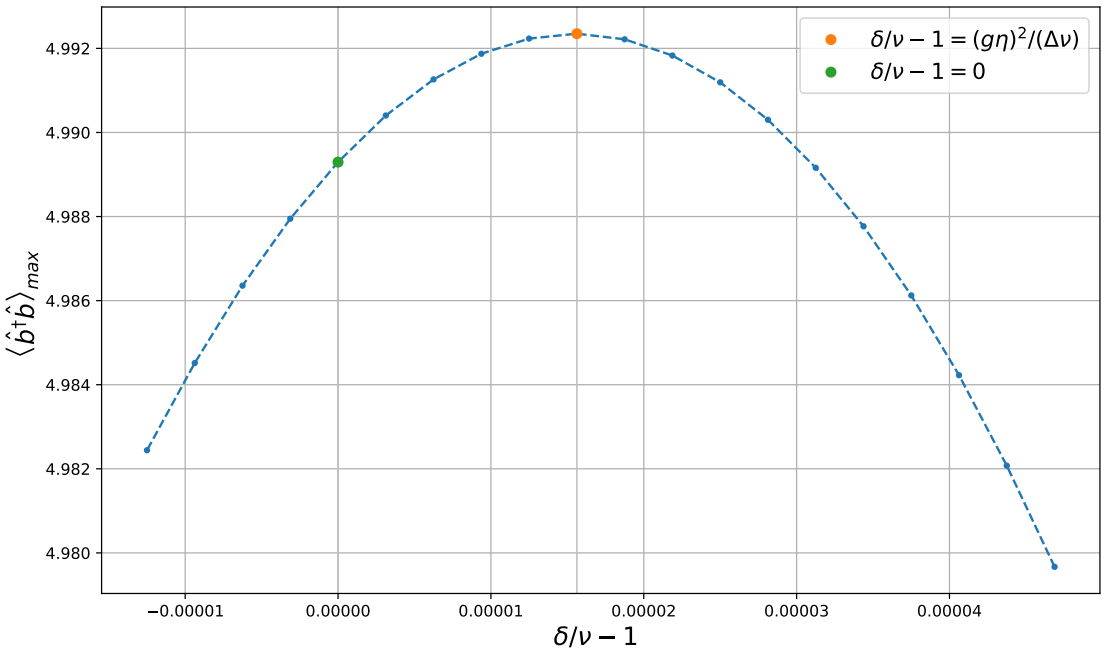

Figure 3: The highest achieved motional occupation $\langle n_m \rangle_{max} = \left\langle \hat{b}^\dagger \hat{b} \right\rangle_{max}$ versus $\delta/\nu - 1$ in the system with 5 quanta of energy. Due to the Stark shift coming from coupling between cavity and motional modes, the perfect resonance is not achieved at $\delta = \nu$ but rather at some other frequency $\delta > \nu$.

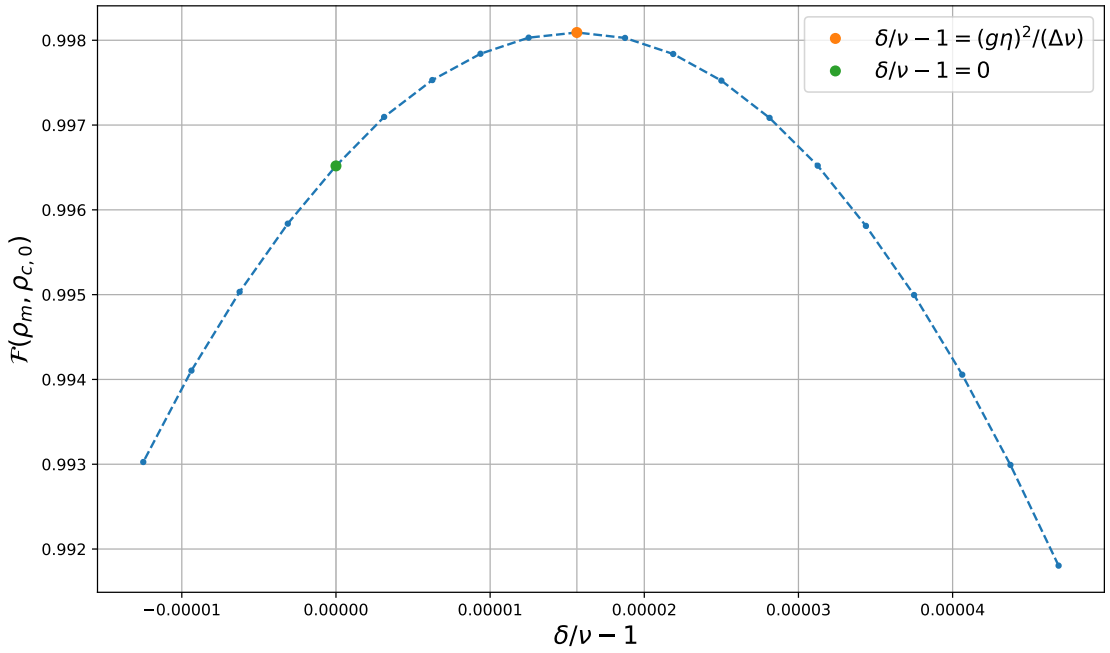

Figure 4: Maximum fidelity $\mathcal{F}\left(\rho_m, \rho_{c,0}\right)$ between reduced density matrix of cavity at time zero $(\rho_{c,0})$ and motion (ρ_m) versus $\delta/\nu - 1$ for transferring the state $|\psi_0\rangle = |5\rangle_{cavity} \otimes |0\rangle_{atom} \otimes |0\rangle_{motion}$. The fidelity stays below 1 as can be expected from Figure 3, because the transfer of population is not perfect. The reasons are higher order terms in Schrieffer-Wolf transformation, off-resonant excitation of the blue sideband and motional relaxation terms produced by the red sideband.

4.2 Higher Fock states

At higher Fock states the fidelities and maximum motional occupation decreases, which will be observed in a transfer of Fock state 15 from cavity to motional modes (the dimension of the Hilbert space we use in simulation is 20). Fidelities on Figure 5a compared to Figure 3 are lower by more than 0.01 (1%). This is no surprise because the relative number of transferred excitations is lower, which can be observed on Figure 5b. The reason is higher order terms in Schrieffer-Wolf transformation. If we compare Fock and cat states, maximum fidelity of Fock state transfer is correctly predicted by equation (8). Fock states do not have precisely defined phase therefore stark shift will not affect the phase as it does with cat states.

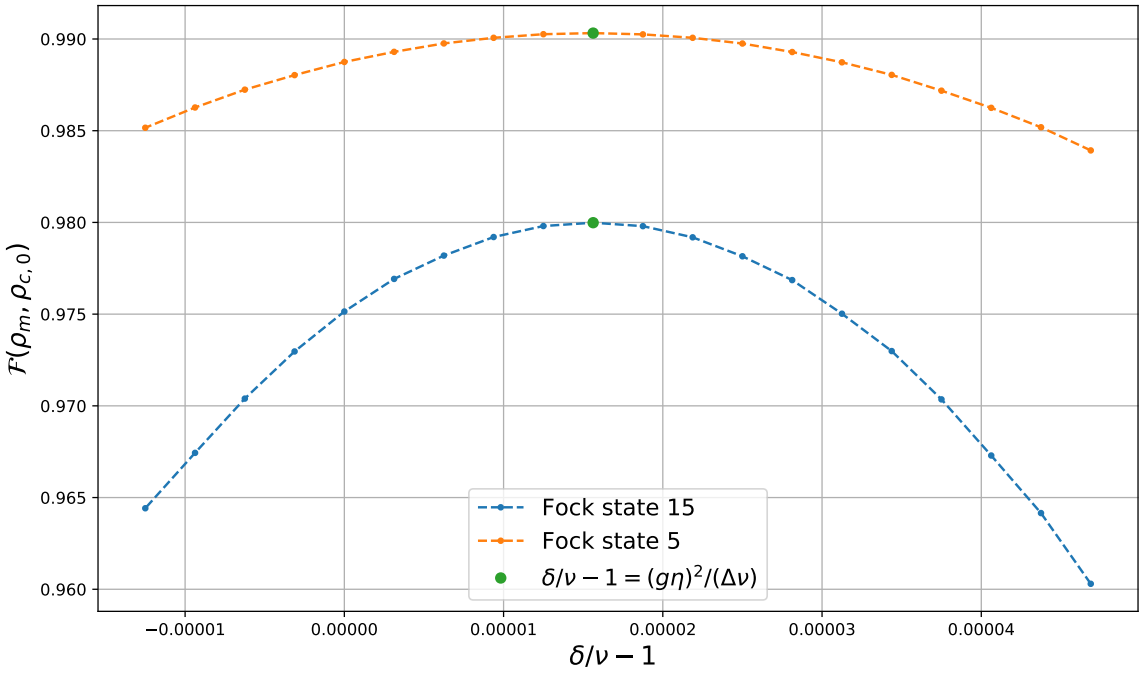

(a)

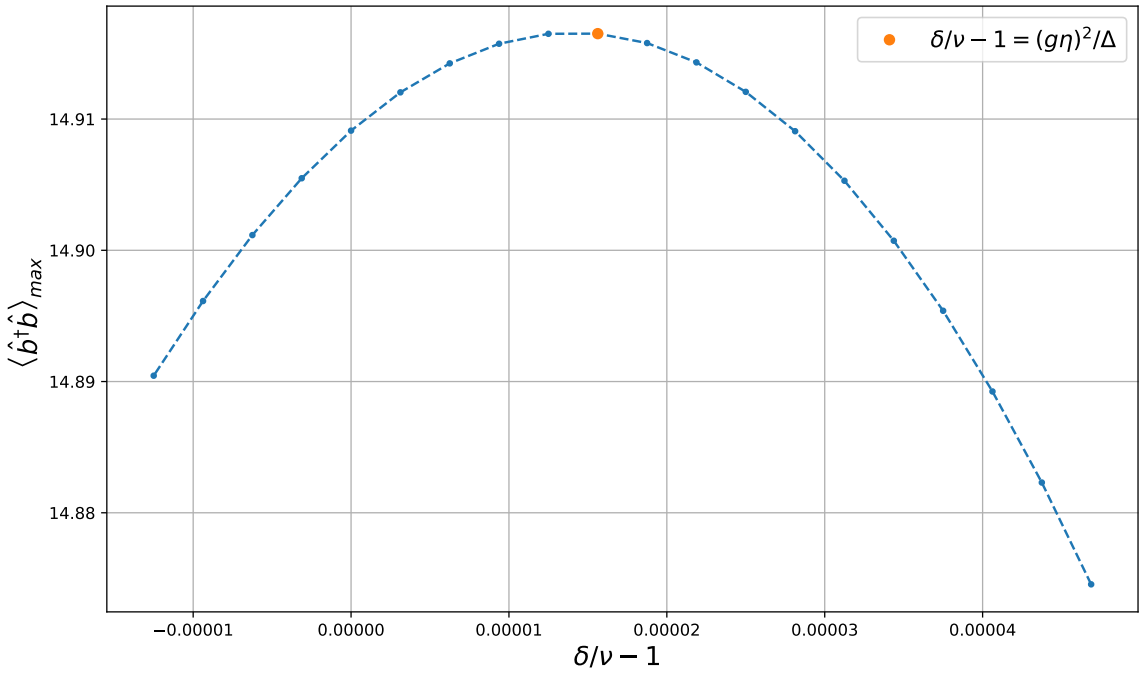

(b)

Figure 5: Maximum fidelity (a) and the highest motional occupation number (b) with respect to $\delta/\nu - 1$. If we compare the two lines for Fock state 5 and Fock state 15, we can observe that the quality of state transfer for Fock state 15 is lower than for Fock state 5 due to higher order terms in Schrieffer-Wolf transformation.

4.3 Cat states

We initialize our system in the state $1/N \cdot \left(|\alpha = 1\rangle + |\alpha = -1\rangle\right)_{cavity} \otimes |0\rangle_{spin} \otimes |0\rangle_{motion}$, where for cavity $|\alpha = 1\rangle$ and $|\alpha = -1\rangle$ denote coherent states 1 and -1 respectively, while for spin and motion $|M\rangle$ means Fock state M (additionally a factor N comes from normalization). We get time evolution of expected occupation number in Figure 6.

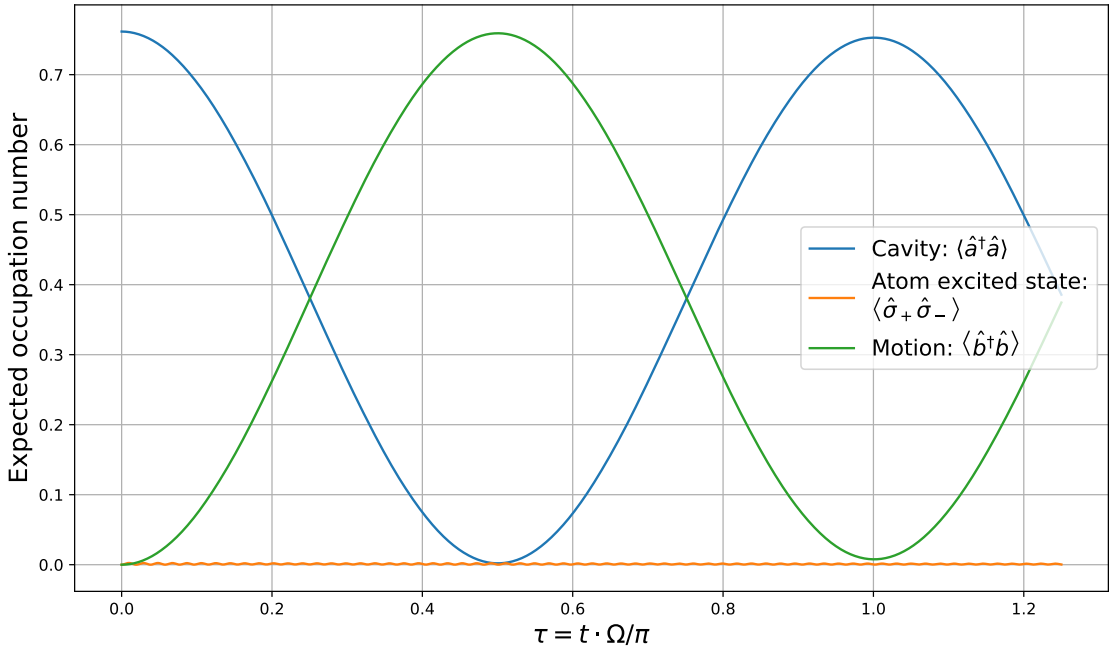

Figure 6: Time evolution of cavity, motion and spin population if the initial state is $1/N \cdot \left(|\alpha = 1\rangle + |\alpha = -1\rangle\right)_{cavity} \otimes |0\rangle_{spin} \otimes |0\rangle_{motion}$

By doing a partial trace on the density matrix of the full system which includes cavity, motion and spin degrees of freedom, we get the density matrix of a particular component of our system. When the expected motional occupation number $\left\langle \hat{b}^\dagger \hat{b} \right\rangle$ is the largest (this happens at $\tau = 0.5$), we do a partial trace and plot the Wigner function in the frame rotating at the frequency of the harmonic trap ν in Figure 7a. We have used the transformation $\rho_m \to U^\dagger(t) \rho_m U(t)$ with $U(t) = \exp\left(-\mathrm{i}\nu t \hat{b}^\dagger \hat{b}\right)$ to move into the frame rotating at the trap frequency. We rotate the state by $\pi/2$ which is a phase gained by unitary evolution of Hamiltonian $\hbar\Omega\left(\hat{a}^\dagger \hat{b} + \hat{a}\hat{b}^\dagger\right)$ for time $\tau = 1/2$ and get Figure 7c. It can be compared with the initial state of the cavity (the state we want to transfer to the motion) on Figure 7b. We can notice that picture 7c is not symmetric under the reflection over the imaginary axis, but is slightly rotated (and distorted) compared to 7b. We can improve this by taking into account the Stark shift.

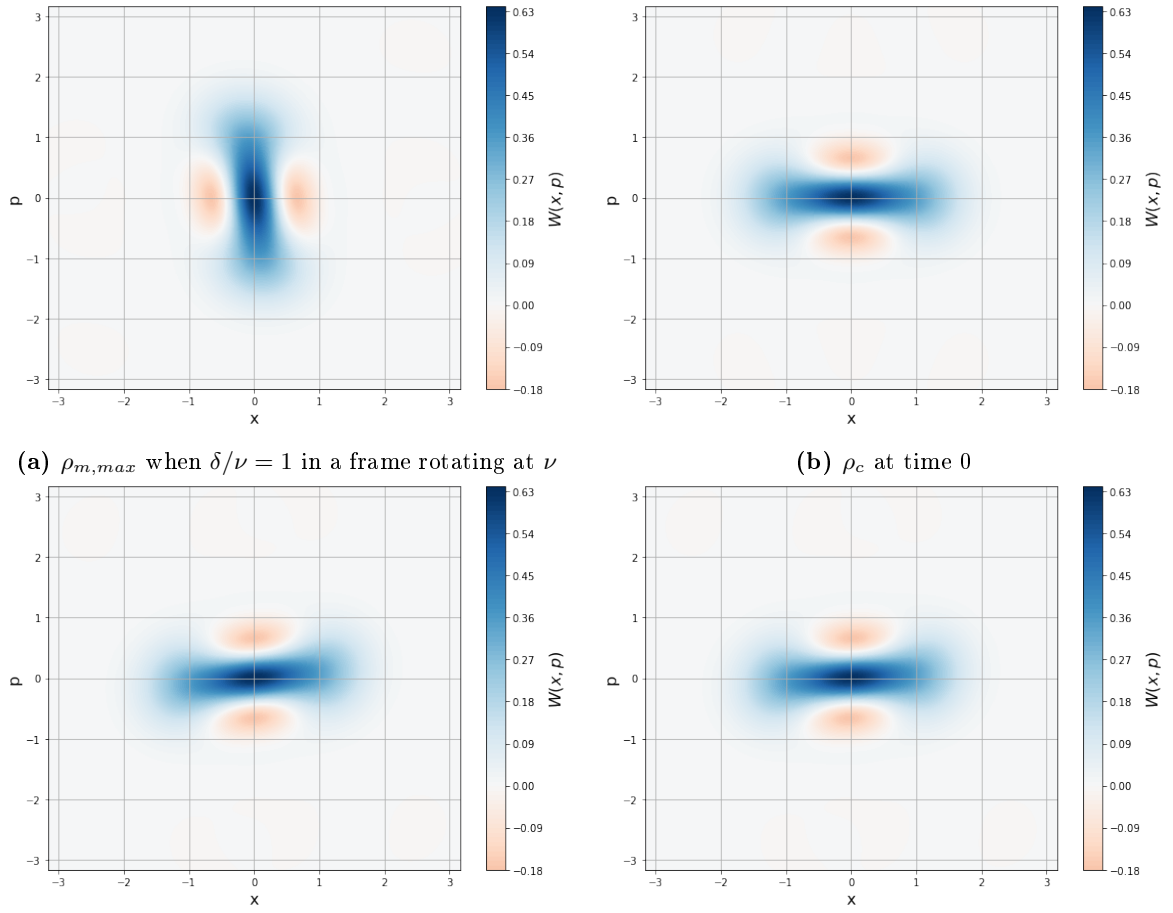

(a) $\rho_{m,max}$ when $\delta/\nu = 1$ in a frame rotating at ν

(b) ρ_c at time 0

(c) Plot from Figure 7a rotated by $\pi/2$

(d) $\rho_{m,max}$ when $\delta/\nu = 1 + (g\eta)^2/(\Delta\nu)$ in a frame rotating at ν and rotated by $\pi/2$

Figure 7: Plots of Wigner function for different density matrices. The color scale on the right represents the values of a Wigner function $W(x,p)$, where for reduced motional density matrix x and p are dimensionless position and momentum: $\hat{x} = 1/2 \cdot \left(\hat{b}^\dagger + \hat{b}\right)$, $\hat{p} = \mathrm{i}/2 \cdot \left(\hat{b}^\dagger - \hat{b}\right)$. Analogously, for reduced cavity density matrix x and p are field quadratures: $\hat{x} = 1/2 \cdot \left(\hat{a}^\dagger + \hat{a}\right)$, $\hat{p} = \mathrm{i}/2 \cdot \left(\hat{a}^\dagger - \hat{a}\right)$. (a) Wigner function of the reduced motional density matrix when the motional occupation number is the highest $\rho_{m,max}$ at $\delta/\nu = 1$. This is in a frame rotating at the trap frequency. We can notice a shift of $\pi/2$ which comes from the beamsplitter interaction. (b) Wigner function of the reduced cavity density matrix at time 0. (c) The Wigner function from Figure (7a) rotated by $\pi/2$ so that we can compare it to (7b). (d) Wigner function of the reduced motional density matrix for $\delta/\nu = 1+(g\eta)^2/(\Delta\nu)$ in the frame rotating at the trap frequency and rotated by $\pi/2$. The resemblance to Figure 7b is higher than resemblance of Figures 7b and 7c which means that accounting for the Stark shift improved our fidelity.

We vary $\delta/\nu - 1$ (near the value $\delta \approx \nu$) and try to find the best fidelity and highest motional occupation in Figure 8 for two different Hamiltonians. One Hamiltonian (blue color) includes off-resonant excitations (which are small when δ is near ν, but would be resonant when $\delta \approx -\nu$) in the interaction part (last term) of equation (3): $\left(\hat{b} + \hat{b}^\dagger\right)\left(\hat{a}\hat{\sigma}_+ + \hat{a}^\dagger\hat{\sigma}_-\right)$. The other (green color) only has resonant terms: $\hat{a}^\dagger\hat{\sigma}_-\hat{b} + \hat{a}\hat{\sigma}_+\hat{b}^\dagger$. In Figure 8a we can see that equation (8) corresponds to the maximum of the highest achieved motional occupation. To calculate the fidelity, we take the partial density matrix of motion when the motional occupation number is the highest. The corresponding state is shown on Figure 7a. Then we rotate the plot by phase gained due to beamsplitter interaction which is $\pi/2$

(Figure 7c) and calculate the fidelity with respect to the initial state in the cavity on Figure 7b. The fidelity we get is plotted on Figure 7b.

The Hamiltonian with off-resonant terms included produces lower quality state transfer, because additional blue sideband terms that do not conserve energy are present as discussed in section 3. For example, the term $\hat{a}\hat{b}$ decreases the total number of excitations and $\hat{a}^\dagger\hat{b}^\dagger$ creates them. They can be suppressed by making δ larger. The fidelity at $\delta/\nu - 1 = (g\eta)^2/(\Delta\nu)$ for the resonant Hamiltonian is 1‰ higher compared to the off-resonant Hamiltonian which can be used as an estimate of how blue sideband terms affect fidelity. The Hamiltonian with only resonant terms also has fidelity below 1 due to higher order corrections in Schrieffer-Wolf transformation. However, the previously performed transformation is different for the resonant Hamiltonian due to the lack of $\hat{a}\hat{b}\hat{\sigma}_+ + \hat{a}^\dagger\hat{b}^\dagger\hat{\sigma}_-$ in the interaction part.

Regardless of the Hamiltonian our prediction from equation (8) corresponds to the maximum in Figure 8a, and is slightly incorrect for Figure 8b, because the state is still rotated (and asymetric) even when accounting for Stark shift caused by red sideband interaction as visible on Figure 7d. The reasons for rotation are higher order corrections in Schrieffer-Wolf transformation, the blue sideband Stark shift and errors caused by $\hat{a}^\dagger\hat{a}\left(\hat{b}^2 + \left(\hat{b}^\dagger\right)^2\right)$ terms. The phase of our state becomes more similar to the initial state of cavity if the detuning δ/ν is slightly higher than predicted and fidelity goes up. The results can be interpreted visually. The Wigner function for $\delta/\nu = 1 + (g\eta)^2/(\Delta\nu)$ is plotted in Figure 7d. The similarity to state on Figure 7b is higher than similarity of density matrix when $\delta/\nu = 1$ (Figure 7c), so our fidelity is better.

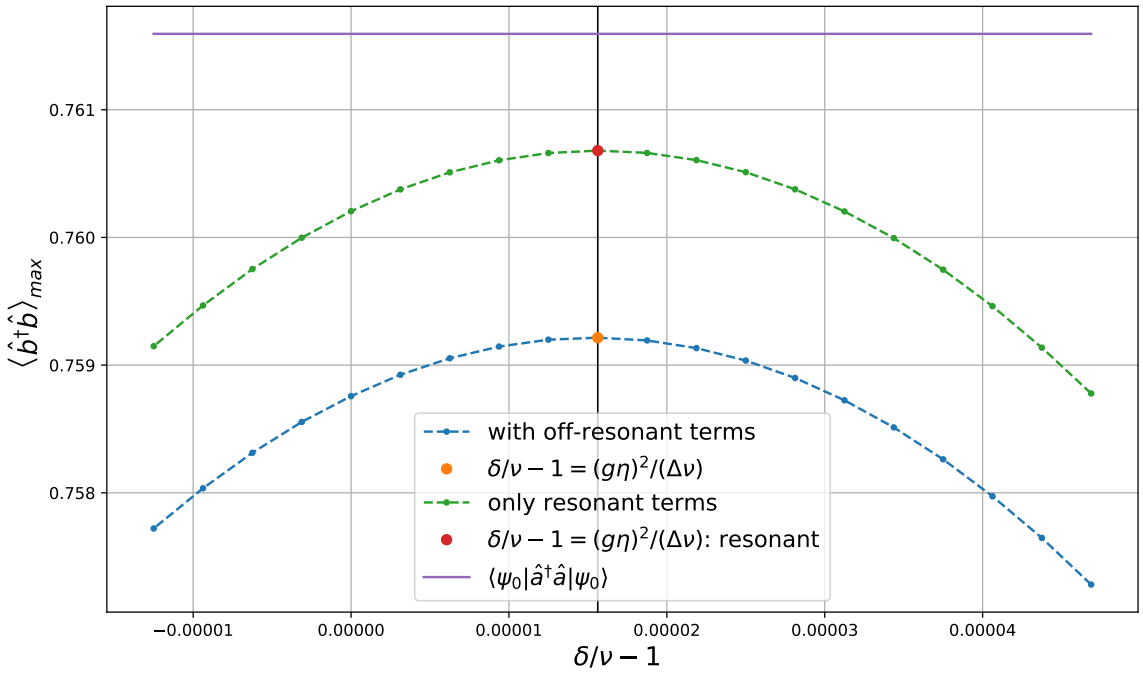

(a)

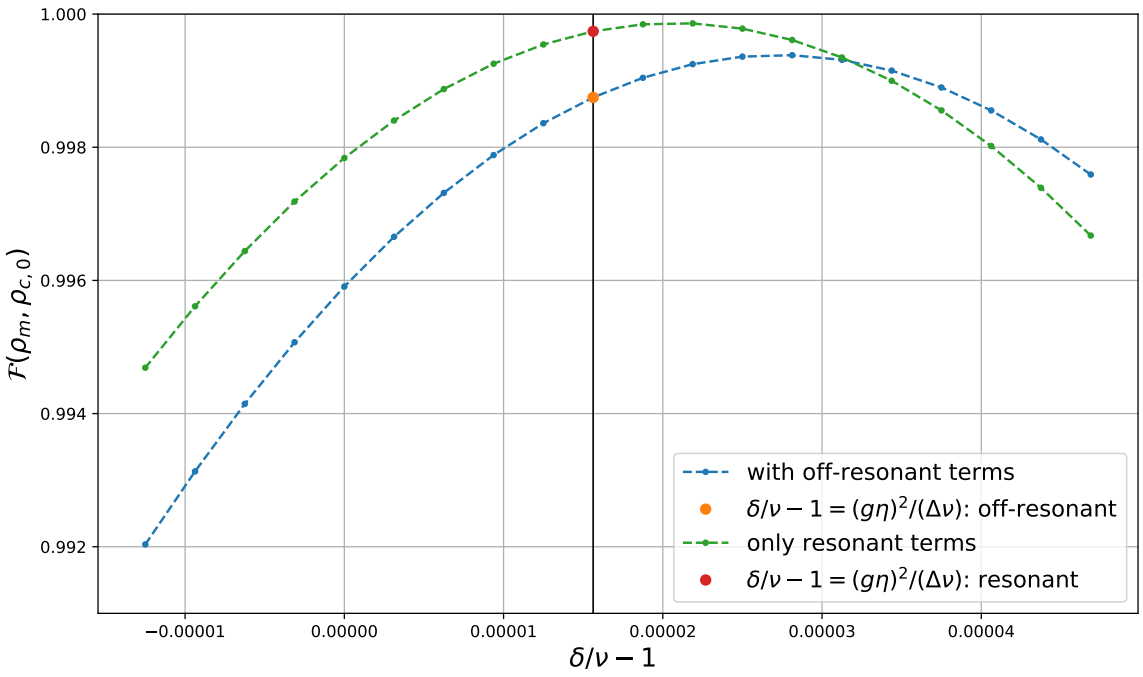

(b)

Figure 8: We initialize our system in: $1/N \cdot \left(|1\rangle + |-1\rangle\right)_{cavity} \otimes |0\rangle_{spin} \otimes |0\rangle_{motion}$ and observe dynamics of two different Hamiltonians. One includes only resonant terms in the interaction part: $\hat{a}^\dagger\hat{\sigma}_-\hat{b} + \hat{a}\hat{\sigma}_+\hat{b}^\dagger$ and is colored green. The other has additional off resonant terms: $\left(\hat{b} + \hat{b}^\dagger\right)\left(\hat{a}\hat{\sigma}_+ + \hat{a}\hat{\sigma}_-^\dagger\right)$ and is shown in blue.
We look at two plots: (a) The highest expected motional occupation number versus $\delta/\nu - 1$ (b) Fidelity of the state with highest motional occupation number with respect to $\delta/\nu - 1$. The maximum of fidelities does not correspond to maximum of occupation number, which is due to higher order terms in Schrieffer-Wolf transformation. Consequently, the states are still deformed a little when the energy transfer reaches maximum. The alignment with initial state gets better at higher $\delta/\nu - 1$ even though the maximum population is smaller and this contributes to better fidelity. We can conclude that off-resonant terms reduce the quality of state transfer which can be expected from section 3.

5 State transfer between two cavities and motion

We can expand our system by unidirectionally coupling (this can be achieved with the use of Faraday isolators) a new cavity (also referred to as the "second cavity") to the already existing cavity in our system as can be seen on Figure 9.

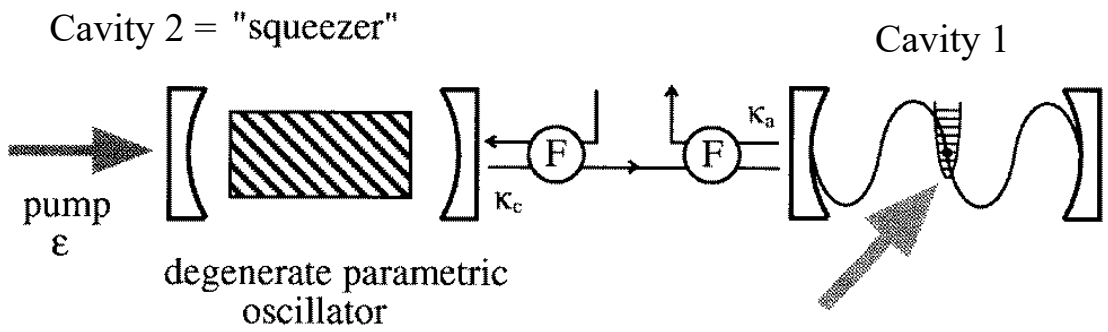

Figure 9: A picture of our setup for generating squeezed states in the motional modes of an ion. Instead of the parametric oscillator, one could also use different drive (for example coherent) to generate a different state.
Taken from [14].

The equation describing time evolution of the total density matrix ρ is [14]:

$$\frac{\mathrm{d}\rho}{\mathrm{d}t} = -\frac{\mathrm{i}}{\hbar}\left[\hat{H}_{ab}+\hat{H}_c,\rho\right]+\kappa_a(2a\rho a^\dagger - a^\dagger a\rho - \rho a^\dagger a)+\kappa_c(2c\rho c^\dagger - c^\dagger c\rho - \rho c^\dagger c)-2\sqrt{\kappa_a\kappa_c}\left(\left[a^\dagger, c\rho\right]+\left[\rho c^\dagger, a\right]\right). \tag{12}$$

Here H_{ab} describes effective beamsplitter coupling between motion of the ion and cavity light field as derived in [14]. We can also arrive at the same interaction terms by taking only the first order terms in η in equations (6), (9). Then we go into the interaction picture with respect to bare Hamiltonians of harmonic trap and cavity and arrive at:

$$\hat{H}_{ab} = \hbar\Omega\left(\hat{a}^\dagger\hat{b}+\hat{a}\hat{b}^\dagger\right)+\hbar\Omega\left(\hat{a}^\dagger\hat{b}^\dagger \mathrm{e}^{2\mathrm{i}\nu t}+\hat{a}\hat{b}\mathrm{e}^{-2\mathrm{i}\nu t}\right). \tag{13}$$

The Hamiltonian of our second (driven) cavity is labeled as $\hat{H}_c$. For example to simulate generation of coherent states one should use $\hat{H}_c = \hbar\omega\left(\hat{c}+\hat{c}^\dagger\right)$. Operator $\hat{a}$ is annihilation operator of the cavity field in the first cavity and $\hat{c}$ is the annihilation operator in the second cavity. The first term in equation (12) describes the unitary evolution of our system, the second and third term are non-unitary and represent decay of first cavity at decay rate κ_a and second cavity at the rate κ_c. The source of decay is thermalisation of the cavity mode. The last two terms describe the coupling between two cavities and are non-unitary, which is a consequence of breaking the reflection invariance of our system with the use of Faraday isolators (light can only travel in one direction from cavity 2 to cavity 1) [19].

Generation of non classical states of motion

We assume (as in [14]) that our second cavity confines a parametric oscillator used to generate squeezed states of light. The corresponding Hamiltonian with ϵ being the amplitude of coherent field driving the oscillator is:

$$\hat{H}_c = \frac{1}{2}\mathrm{i}\hbar\left(\epsilon^*\hat{c}^2-\epsilon\left(\hat{c}^\dagger\right)^2\right). \tag{14}$$

The parameters for our simulation are taken from [14] (up to the arbitrary choice of κ_a since only the ratios with respect to κ_a were given): $\nu = 10\cdot 2\pi s^{-1}$, $\omega_c = 10\cdot 2\pi s^{-1}$, $\omega_a = 20\cdot 2\pi s^{-1}$, $\Omega = 0.1\cdot 2\pi s^{-1}$,

$\kappa_a = \kappa_c = 1 \cdot 2\pi s^{-1}$, $\epsilon = 0.3 \cdot 2\pi s^{-1}$. The steady state of motion is approached on a timescale $\tau = \kappa_a/\Omega^2$ according to [14]. For our parameters this characteristic time is approximately 4 seconds, so we must make sure to observe our dynamics for longer than this, so that the system reaches a steady state. Time evolution of the ground state of our system with respect to dimensionless time t/τ is plotted in Figure 10.

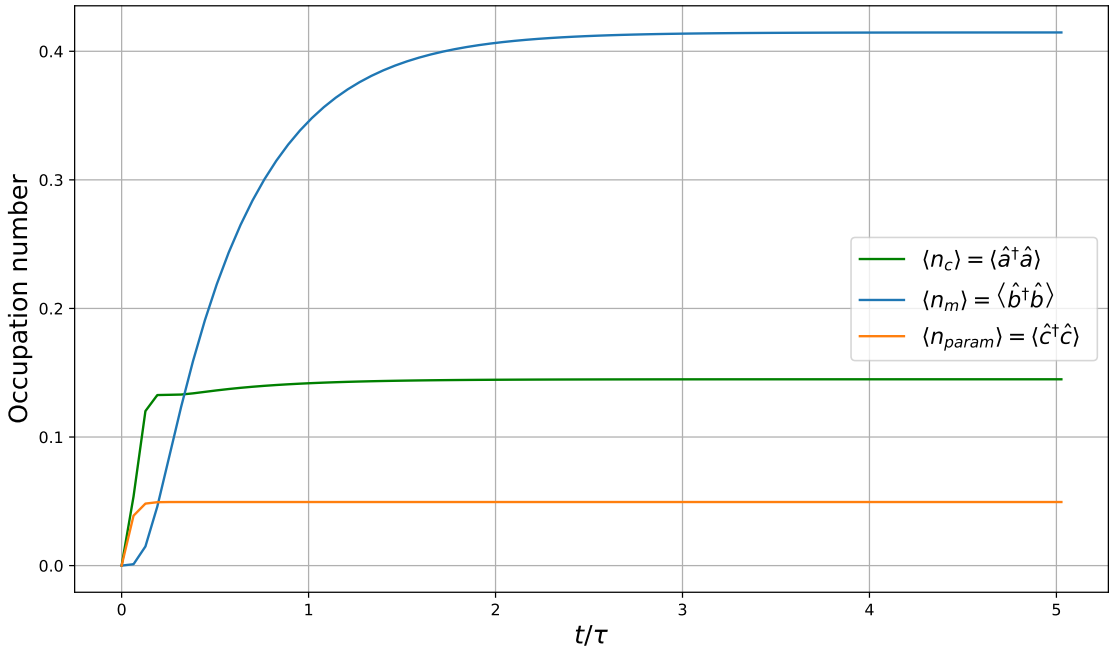

Figure 10: Time evolution of expected occupation numbers for different subsystems if we start in the ground state. A squeezed state is generated in the parametric oscillator, which is unidirectionally coupled to the cavity via decay. The state from cavity is then further transferred to the motional mode through the beamsplitter-like coupling.

To check if our parametric oscillator really produced a squeezed state we can look at the elements of a steady state reduced density matrix of the motional mode in Figure 11. Characteristics of a squeezed vacuum states are evident since only even number states are populated. We can also observe the squeezing by looking at the Wigner function on Figure 12. The squeezing corresponds to the fitted parameters $s = 0.6060$ and $\theta = 3.141$, which we get by maximizing fidelity between reduced density matrix of a motional mode and $\hat{S}\left(se^{i\theta}\right)|0\rangle$ while varying parameters s and θ ($\hat{S}$ is the squeezing operator). The final states in parametric oscillator and cavity are also squeezed.

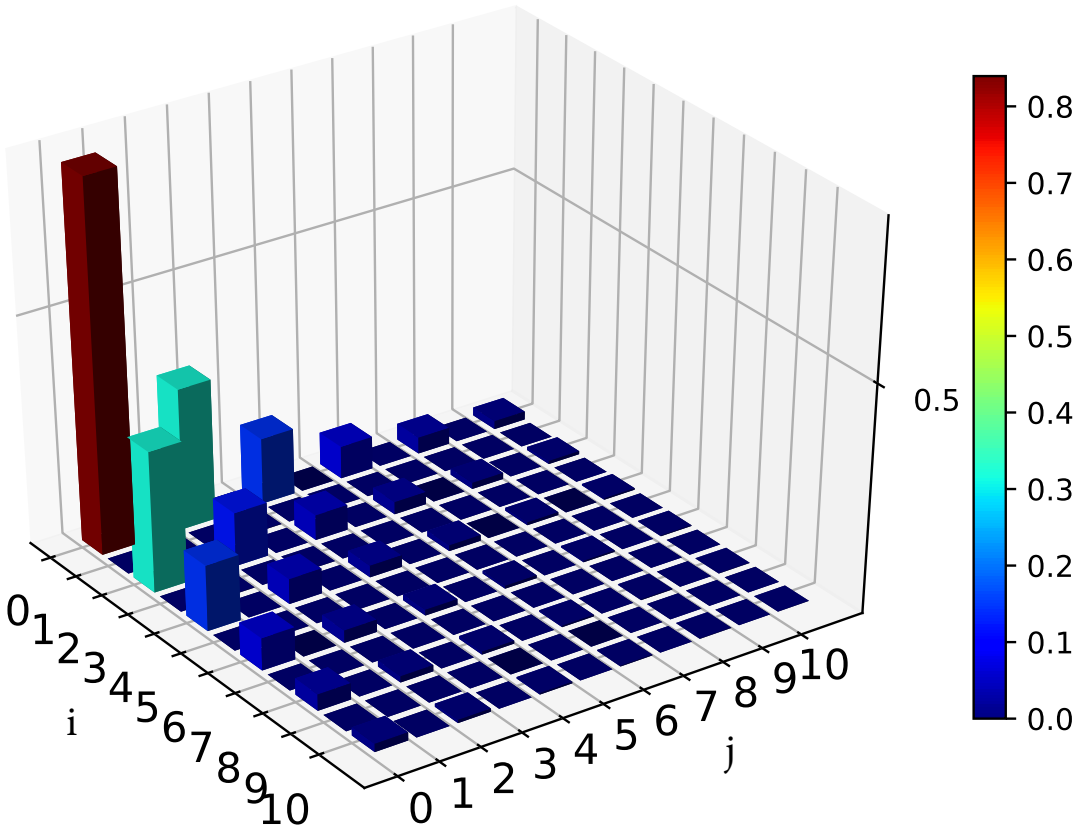

Figure 11: Absolute value of elements of the steady state reduced motional density matrix $\left(\left|(\rho_m)_{i,j}\right|\right)$ when our system is driven by a parametric oscillator. The color bar on the right shows absolute value of matrix elements. We can see that matrix elements with either i or j odd are not populated which is a characteristic of a squeezed vacuum state. The distribution agrees with the one in Kimble's paper [14].

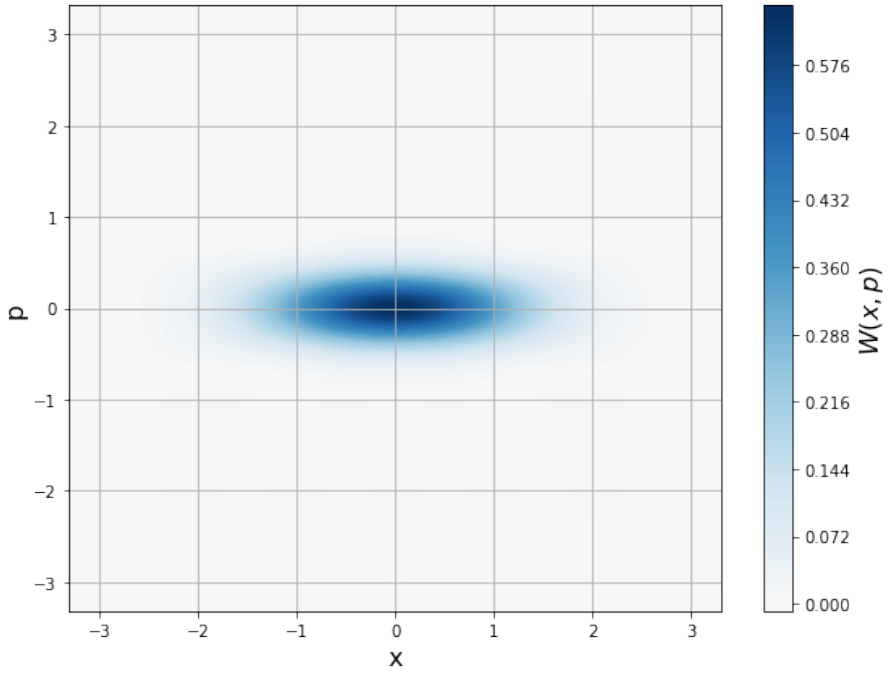

Figure 12: Wigner function $W(x,p)$ of the final state in the motional mode of the ion. x and p are the dimensionless position and momentum: $\hat{x} = 1/2\left(\hat{b}^\dagger + \hat{b}\right)$, $\hat{p} = \mathrm{i}/2\left(\hat{b}^\dagger - \hat{b}\right)$. The squeezing corresponds to squeezed state $\hat{S}\left(s\mathrm{e}^{\mathrm{i}\theta}\right)|0\rangle$ with $s = 0.6060$ and $\theta = 3.141$. The parameters were chosen such that fidelity between steady-state reduced density matrix of motion and squeezed state $\hat{S}\left(s\mathrm{e}^{\mathrm{i}\theta}\right)|0\rangle$ is the highest $\left(\mathcal{F}\left(\rho_m, \hat{S}\left(s\mathrm{e}^{\mathrm{i}\theta}\right)|0\rangle\langle 0|\hat{S}^\dagger\left(s\mathrm{e}^{\mathrm{i}\theta}\right)\right) \approx 0.999\right)$.

We can influence the degree of squeezing by changing the parameter ϵ in equation (14). Dependence of squeezing parameter s relative to ϵ is plotted on Figure 13. Squeezing increases with ϵ.

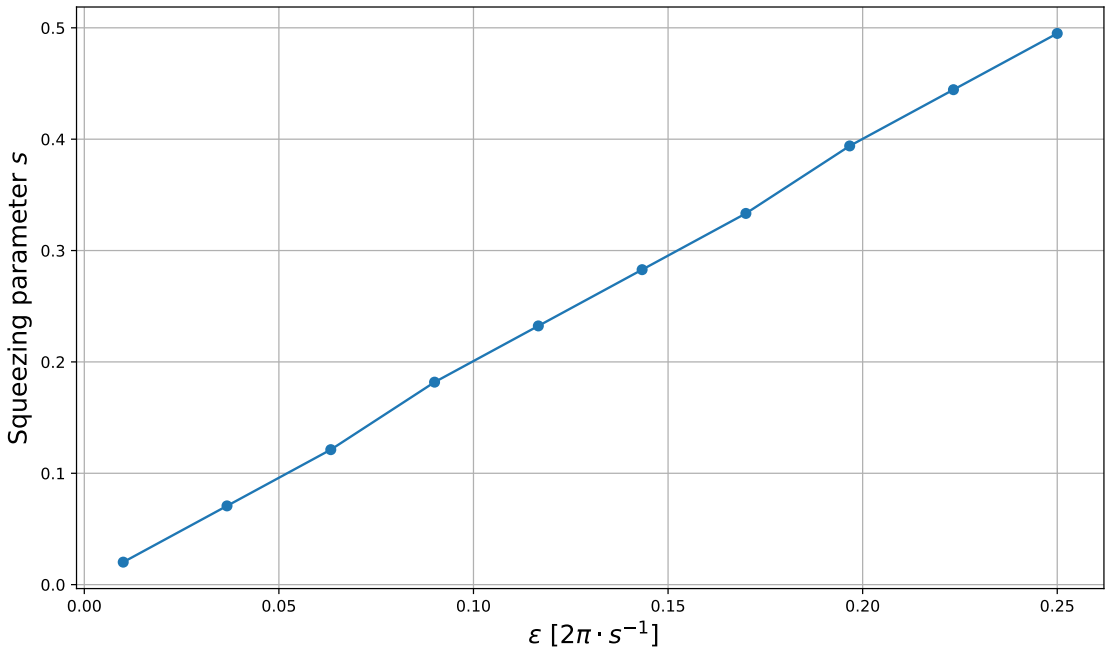

Figure 13: Dependence of squeezing parameter s on the strength of the parametric oscillator ϵ.

6 Conclusion

Optical cavity and motional mode of a trapped ion in a cavity can be coupled by driving internal transition of the two-level ion with a laser beam. This results in beamsplitter-like interaction between cavity and motion which is responsible for state transfer. Other terms reduce fidelity and have to be treated carefully. Firstly, we need to be in a regime where higher order terms of Schrieffer-Wolf transformation can be neglected. Secondly, blue sideband (anti Jaynes-Cummings) terms can be neglected if δ is sufficiently large. Moreover, Stark shift (from red sideband terms) of energy levels should be compensated by the detuning of the laser. If all of this requirements are fulfilled, our state transfer can achieve high fidelities regardless of inevitable errors arising from Lamb-Dicke approximation and slow (second order in Lamb-Dicke parameter) relaxation of the motional state.

After investigating state transfer between cavity and motion of the ion, we proceeded by coupling another cavity (parametric oscillator) to our system and simulated generation of squeezed states of motion. A further step would be to put an ion in the second cavity (which was previously used as parametric oscillator) and investigate state transfer between two physically separated ions. Ultimately this could be beneficial in scaling up quantum computers because photons could mediate coupling between spatially distant qubits.

7 References

[1] D. M. Meekhof, C. Monroe, B. E. King, W. M. Itano, and D. J. Wineland, *Generation of Nonclassical Motional States of a Trapped Atom,* Physical Review Letters 76, 1796 (1996)

[2] J.I.Cirac, A.S.Parkins, R.Blatt, P.Zoller, *Nonclassical States of Motion in Ion Traps* Advances In Atomic, Molecular, and Optical Physics 37, 237 (1996)

[3] C. Monroe, D. M. Meekhof, B. E. King, D. J. Wineland, *"Schrödinger Cat" Superposition State of an Atom,* Science 272, 1131 (1996)

[4] J. I. Cirac and P. Zoller, *Quantum Computations with Cold Trapped Ions*, Physical Review Letters 74, 4091 (1995)

[5] C. Monroe, D. M. Meekhof, B. E. King, W. M. Itano, and D. J. Wineland, *Demonstration of a Fundamental Quantum Logic Gate,* Physical Review Letters 75, 4714, 1995

[6] B. E. King et. al., *Cooling the Collective Motion of Trapped Ions to Initialize a Quantum Register, P*hysical Review Letters 81, 1525 (1998)

[7] Q. A. Turchette, et. al., *Deterministic Entanglement of Two Trapped Ions,* Physical Review Letters 81, 3631, (1998)

[8] I. L. Chuang, D. W. Leung, and Y. Yamamoto, *Bosonic quantum codes for amplitude damping,* Physical Review A 56, 1114 (1997)

[9] M. H. Michael, et al., *New Class of Quantum Error-Correcting Codes for a Bosonic Mode,* Physical Review X 6, 031006 (2016)

[10] A. P. Lund, T. C. Ralph, and H. L. Haselgrove, *Fault-Tolerant Linear Optical Quantum Computing with Small-Amplitude Coherent States,* Physical Review Letters 100, 030503 (2008)

[11] P. T. Cochrane, G. J. Milburn, and W. J. Munro, *Macroscopically distinct quantum-superposition states as a bosonic code for amplitude damping,* Physical Review A 59, 94 (2017)

[12] D. Gottesman, A. Kitaev, J. Preskill, *Encoding a qubit in an oscillator,* Physical Review A 64, 012310 (2001)

[13] J. M. Pino, et. al., *Demonstration of the trapped-ion quantum CCD computer architecture,* 592, 209-213 (2021)

[14] A. S. Parkins and H. J. Kimble, *Quantum state transfer between motion and light,* Journal of Optics B: Quantum and Semiclassical Optics 1, 496 (1999)

[15] S. Bravyi, D. DiVincenzo, D. Loss, *Schrieffer-Wolff transformation for quantum many-body systems,* Annals of Physics 326, 2793 (2011)

[16] *Schrieffer–Wolff transformation*, 27. 6. 2021, Accessible on: https://en.wikipedia.org/wiki/Schrieffer-Wolff_transformation.

[17] J. R. Johansson, P. D. Nation, and F. Nori, *QuTiP: An open-source Python framework for the dynamics of open quantum systems.*, Comp. Phys. Comm. 183, 1760–1772 (2012)

[18] *Autler–Townes effect*, 27. 6. 2021, Accessible on: https://en.wikipedia.org/wiki/Autler-Townes_effect.

[19] C. W. Gardiner, *Driving a quantum system with the output field from another driven quantum system*, Physical Review Letters 70, 2269 (1993)